Short temporal coherence digital holography with a femtosecond frequency comb laser for multi-level optical sectioning

Klaus Körner,[1,*] Giancarlo Pedrini,[1] Igor Alexeenko,[1] Tilo Steinmetz,[2] R. Holzwarth,[2] and W. Osten[1]

[1]Institut für Technische Optik and Research Center SCoPE, Pfaffenwaldring 9, Universitaet Stuttgart,70569 Stuttgart, Germany
[2]MenloSystems GmbH, Martinsried, Germany
**koerner@ito.uni-stuttgart.de*

Abstract: In this paper, we demonstrate how short temporal coherence digital holography with a femtosecond frequency comb laser source may be used for multi-level optical sectioning. The object shape is obtained by digitally reconstructing and processing a sequence of holograms recorded during stepwise shifting of a mirror in the reference arm. Experimental results are presented.

OCIS codes: (090.0090) Holography; (090.1995) Digital holography; (120.3940) Metrology; (140.3538) Lasers pulsed.

References and links

1. J. W. Goodman and R. W. Lawrence, “Digital image formation from electronically detected holograms,” Appl. Phys. Lett. **11**(3), 77–79 (1967).
2. W. S. Haddad, D. Cullen, J. C. Solem, J. W. Longworth, A. McPherson, K. Boyer, and C. K. Rhodes, “Fourier-transform holographic microscope,” Appl. Opt. **31**(24), 4973–4978 (1992).
3. U. Schnars, “Direct phase determination in hologram interferometry with use of digitally recorded holograms,” J. Opt. Soc. Am. A **11**(7), 2011–2015 (1994).
4. I. Yamaguchi and T. Zhang, “Phase-shifting digital holography,” Opt. Lett. **22**(16), 1268–1270 (1997).
5. C. Wagner, S. Seebacher, W. Osten, and W. Jüptner, “Digital recording and numerical reconstruction of lensless Fourier holograms in optical metrology,” Appl. Opt. **38**(22), 4812–4820 (1999).
6. C. Wagner, W. Osten, and S. Seebacher, “Direct shape measurement by digital wavefront reconstruction and multiwavelength contouring,” Opt. Eng. **39**(1), 79–85 (2000).
7. L. Martínez-León, G. Pedrini, and W. Osten, “Applications of short-coherence digital holography in microscopy,” Appl. Opt. **44**(19), 3977–3984 (2005).
8. Y. C. Lin, C.-J. Cheng, and T. C. Poon, “Optical sectioning with a low-coherence phase-shifting digital holographic microscope,” Appl. Opt. **50**(7), B25–B30 (2011).
9. C. Yuan, H. Zhai, X. Wang, and L. Wu, “Lensless digital holography with short coherence light source for three-dimensional surface contouring of reflecting micro objects,” Opt. Commun. **270**(2), 176–179 (2007).
10. T. Udem, R. Holzwarth, and T. W. Hänsch, “Optical frequency metrology,” Nature **416**(6877), 233–237 (2002).
11. P. Del’Haye, A. Schliesser, O. Arcizet, T. Wilken, R. Holzwarth, and T. J. Kippenberg, “Optical frequency comb generation from a monolithic microresonator,” Nature **450**(7173), 1214–1217 (2007).
12. T. J. Kippenberg, R. Holzwarth, and S. A. Diddams, “Microresonator-based optical frequency combs,” Science **332**(6029), 555–559 (2011).
13. S. Hyun, Y.-J. Kim, Y. Kim, and S.-W. Kim, “Absolute distance measurement using the frequency comb of a femtosecond laser,” CIRP Annals Manufacturing Technology **59**(1), 555–558 (2010).
14. S. Choi, M. Yamamoto, D. Moteki, T. Shioda, Y. Tanaka, and T. Kurokawa, “Frequency-comb-based interferometer for profilometry and tomography,” Opt. Lett. **31**(13), 1976–1978 (2006).
15. T. Steinmetz, T. Wilken, C. Araujo-Hauck, R. Holzwarth, T. W. Hänsch, L. Pasquini, A. Manescau, S. D’Odorico, M. T. Murphy, T. Kentischer, W. Schmidt, and T. Udem, “Laser frequency combs for astronomical observations,” Science **321**(5894), 1335–1337 (2008).
16. T. Wilken, C. Lovis, A. Manescau, T. Steinmetz, L. Pasquini, G. Lo Curto, T. W. Hänsch, R. Holzwarth, and T. Udem, “High-precision calibration of spectrographs,” Mon. Not. R. Astron. Soc. **405**(1), L16–L20 (2010).
17. D. Wei, S. Takahashi, K. Takamasu, and H. Matsumoto, “Analysis of the temporal coherence function of a femtosecond optical frequency comb,” Opt. Express **17**(9), 7011–7018 (2009).
18. J. Schwider, “Multiple beam Fizeau interferometer with filtered frequency comb illumination,” Opt. Commun. **282**(16), 3308–3324 (2009).

#161359 - $15.00 USD Received 11 Jan 2012; revised 23 Feb 2012; accepted 12 Mar 2012; published 14 Mar 2012

19. K. Körner, G. Pedrini, C. Pruss, and W. Osten, German patent application 10 2011 016 660 (to be published).
20. M. Born and E. Wolf, *Principles of Optics,* 7nd ed. (Cambridge University Press, 2011), Chap. 10.
21. J. W. Goodman, *Introduction to Fourier Optics,* 2nd ed. (McGraw-Hill, 1988), Chap. 2.
22. A. Ruehl, A. Marcinkevicius, M. E. Fermann, and I. Hartl, "80 W, 120 fs Yb-fiber frequency comb," Opt. Lett. **35**(18), 3015–3017 (2010).

1. Introduction

Already in 1967 Goodman [1] has shown that holograms may be recorded by optoelectronic devices and the physical reconstruction may be replaced by a numerical reconstruction using a computer. Nowadays, thanks to electronic sensors (CCD, CMOS) and to modern computer resources, the processing of holograms can be performed in a very short time [2–4]. Different methods based on digital holography have been developed for the measurement of the shape of smooth or rough objects. In one of these approaches, the phase difference obtained from the reconstructions of digital holograms which were recorded while the sample is illuminated by different wavelengths is used to calculate the 3-d shape of the object [5,6]. Short coherence digital holography may be used as well for depth sectioning, in this case the interference between the object and reference wave is observed only when their optical path lengths are matched within the coherence length of the laser. The numerical reconstruction of the hologram corresponds to a defined layer in space. The selection of the reconstructed plane can be simply performed by mechanical shifting of a mirror which changes the path difference between object and reference beam. Sectional images of microscopic samples are reported in Refs. 7,8. Instead of a short coherence laser, a femtosecond pulsed laser can be used [9]. This light source emits continuously distributed optical frequencies over a spectral bandwidth $\Delta\nu$, thus we obtain interference only in a narrow range having $c/\Delta\nu$ depth, where the path lengths of the object and reference light match each other (c is the speed of light). In this case too, it will be necessary to scan along the whole depth of the object in order to recover the 3-d shape.

Since several years, the femtosecond frequency comb laser (fc-laser) is applied as an optical frequency synthesizer [10]. Further developments led to the generation of microresonator-based frequency combs [11,12]. The fc-laser has been already used for interferometrical absolute distance measurements [13], profilometry and tomography [14] and has attracted considerable attention for applications in astronomy [15,16]. The analysis of the temporal coherence function of a fc laser shows a strong periodical function that can be used for optical metrology [17]. The application of a multiple beam Fizeau interferometer with filtered frequency comb illumination produced by a Fabry-Pérot cavity has been experimentally demonstrated for surface profiling [18].

In this paper we show how a fc-laser may be used in an arrangement based on digital holography [19]. This light source delivers an elegant approach for the multiple sectioning of the object under investigation. In contrast to conventional approaches, each hologram reconstructs not only the section of the object where reference and object beam matches, but as well other planes with equidistant intervals.

2. Set-up

The set-up for digital holography with a fc-laser, is shown in Fig. 1. The laser beam is at first expanded and collimated by a telescope and later divided into two parts by a beamsplitter. The reflected beam is directed towards the object and the transmitted beam is reflected by a spherical mirror producing a reference wave originating from a point F. The wavefronts reflected by the object and the mirror are recombined by the beamsplitter. The CCD camera records the intensity due to their superposition which may be written as:

$$\begin{aligned} I(Q) = I_R(Q) + 2 \int\limits_{A,A'} \sqrt{I(P,Q)}\sqrt{I(P',Q)}\,\mathrm{Re}\left\{\gamma[(d_{SPQ} - d_{SP'Q})/c]\right\} dA dA' \\ + 2\sqrt{I_R(Q)}\int\limits_{A} \sqrt{I(P,Q)}\,\mathrm{Re}\left\{\gamma[(d_{SRQ} - d_{SPQ})/c]\right\} dA, \end{aligned} \tag{1}$$

where *P* and *Q* are points on the object surface and the CCD plane, respectively. $I_R(Q)$ denotes the intensity of the reference wave at *Q*. The second term describes the interference resulting from the cross correlation between the light coming from different object points *P* and *P'*; d_{SPQ} - $d_{SP'Q}$ is the path difference between source and detector point for two beams reflected by *P* and *P'*. Re{γ} is the real part of the complex degree of coherence γ, *dA* and *dA'* are surface elements over *P* and *P'* respectively. The third term describes the interference between light coming from the object and the reference. d_{SRQ} is the path length of the reference beam starting from the source and ending at the detection point *Q*; d_{SPQ} is the path length of the object beam reflected by the point *P*. The first and the second terms on the right hand side of Eq. (1) do not contain interferences between object and reference and thus are not relevant for the holographic reconstruction. The real part of the complex degree of coherence in the third term can be written as [20]:

$$\mathrm{Re}\left\{\gamma(\tau)\right\} = \left|\gamma(\tau)\right| \cos\left\{\alpha(\tau) - 2\pi(d_{SRQ} - d_{SPQ})/\lambda_0\right\}, \tag{2}$$

where $\tau = (d_{SRQ} - d_{SPQ})/c$, $|\gamma(\tau)|$ is responsible for the contrast of the interference fringes, $2\pi(d_{SRQ} - d_{SPQ})/\lambda_0$ is the phase resulting from the path difference and λ_0 is the mean wavelength of the laser. The degree of temporal coherence $|\gamma(\tau)|$of the frequency comb source can be determined by taking the Fourier Transform of its spectrum $S(\nu)$ which is given by [17]:

$$\left|\gamma(\tau)\right| \propto \left|\mathrm{FT}\left\{\mathrm{S}(\nu)\right\}\right| = \left|\mathrm{FT}\left\{\mathrm{E}(\nu - \nu_0)\right\} \otimes \sum\nolimits_{n=-N}^{N} \delta\left(\tau - \frac{n}{\Delta\nu_{fc}}\right)\right|. \tag{3}$$

FT and $\otimes$ denote a Fourier transform and a convolution operation, respectively. $E(\nu - \nu_0)$, is the envelope with spectral bandwidth $\Delta\nu$; $\nu_0 = c/\lambda_0$, and $\Delta\nu_{fc}$ are the central frequency and the frequency comb spacing of the laser source respectively. $|\gamma(\tau)|$ is a periodic function, displaying peaks separated by $1/\Delta\nu_{fc}$. The peak width ($1/\Delta\nu$) for the frequency comb is very small compared to the pulse separation ($1/\Delta\nu_{fc}$). We may consider that $|\gamma(\tau)| = 0$ between the pulses and by inserting it in Eq. (2), we may obtain interference between the reference and object wave only when the path difference (d_{SRQ} - d_{SPQ}) is equal to *nY*, where *n* is an integer and $Y = c/\Delta\nu_{fc}$ is the spatial pulse separation (see Fig. 1). The interference described by the phase term $2\pi(d_{SRQ} - d_{SPQ})/\lambda_0$ appears not only when the paths match (like in short coherence digital holography) but when the path difference is *nY* as well. This means that by using the arrangement with a fc-laser, we are able to reconstruct different section of the object axially separated by *nY* /2 from a single hologram, successively. The temporal coherence length of one pulse is $c/\Delta\nu \approx 30$ µm and determines the depth of the reconstructed section. By changing the reference path length d_{SRQ} (this can be done by shifting the spherical mirror), we may select which sections of the object are to be reconstructed. The moving mirror is used not only for the axial scanning but to apply the phase-shifting technique as well which is necessary to get the phase of the object wave front [3].

#161359 - \$15.00 USD Received 11 Jan 2012; revised 23 Feb 2012; accepted 12 Mar 2012; published 14 Mar 2012

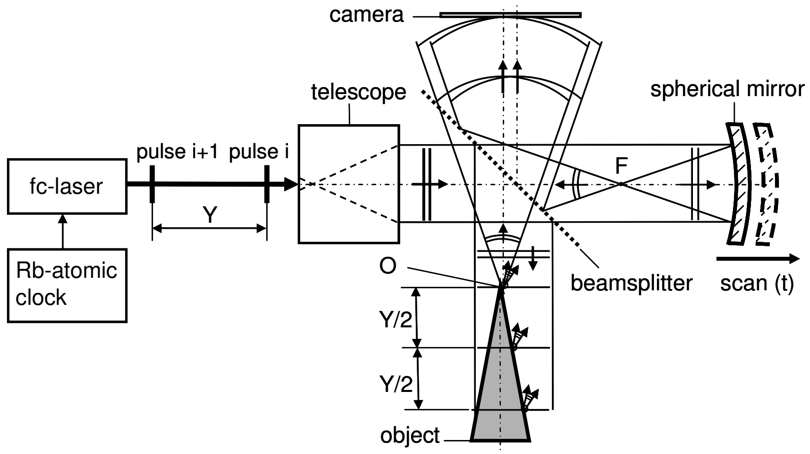

Fig. 1. Experimental set-up for lensless short coherence digital holography [19] with a femtosecond fc-laser at 532 nm, referenced to a Rubidium atomic clock.

3. Experimental results

The Frequency Comb used in the experiment is based on an Yb-doped femtosecond fiber-laser, capable of generating sub-100 fs pulses with a repetition rate of 250 ± 1 MHz and a central wavelength of λ_0 = 1064 nm. The comb's repetition rate and offset frequency is locked to a rubidium atomic clock with an accuracy of 5 parts in 10^{11}. Using Fabry-Pérot-cavities (FPC), the repetition rate of the laser can be increased by a multiple m of the fundamental repetition rate [16]. For the experiments described in this paper, the filter ratio was choosen to be m = 24 resulting in $\Delta\nu_{fc}$ = 5.994 GHz (Y = 50.00 mm). After subsequent amplification in an Yb-doped fiber amplifier and frequency doubling in a LBO crystal, the resulting laser specifications are as follows: pulse duration 100 fs, λ_0 = 532 nm, output power 50 mW, $\Delta\nu$ = 10 THz ($\Delta\lambda\approx$10 nm).

The object used for our investigations is a metallic cone with half angle of 12°, 80 mm coned length and 36 mm base diameter, see. Figure 2(a). A CCD camera (SVS16000) with 4896 x 3280 pixels, pixel size Δ xΔ = 7.4 x 7.4 µm^2, has been used to record the digital holograms which are transferred to the computer by a GigE interface. A reconstruction without aliasing, is possible only when the sampling theorem (see e.g. Refs. 21) is satisfied, this requires to have a band limited intensity distribution with bandwidth less than $1/(2\Delta)$ inside the hologram. This condition is satisfied when the speckle size on the sensor is equal to or larger than the pixel size Δ. In the experiment the distance between the sensor and the object was z = 500 mm and the diameter of the illuminated surface D = 36 mm, thus the speckle size was equal to the pixel size i.e. $\lambda_0 z/D$ = 7.4 µm = Δ. The reference wave originates from the point F, located approximately 500 mm away from the sensor and thus the fringes obtained from the interference between the light coming from the object and the reference have a period which is greater than 2Δ. All the conditions for a reconstruction without aliasing are satisfied. In order to speed up the procedure, only those holograms which were recorded by 3000 x 3000 pixels and covering a detector area L x L = 22 x 22 mm^2 have been evaluated. The lateral resolution of the reconstruction and the depth of field are given by $R_L = \lambda_0/NA$ = 12 µm, and $DF = \lambda_0/NA^2$ = 274 µm, where the numerical aperture in our case can be approximated by $NA = L/z$ = 0.044.

The Figs. 2(b), 2(c), 2(d) show three numerical reconstructions obtained from a single hologram with digital focusing in three different planes, each separated by $Y/2$ = 25.00 mm. In Fig. 2(b), we see a ring with small radius at the center which corresponds to the intersection of the cone with a plane (we will call this PL-1), in the same figure there are two other rings with larger radius describing intersections of the object with two planes (PL-2, PL-3) axially spaced by 25.00 mm and 50.00 mm with respect to PL-1. The three rings appear because we use a frequency comb, in this case $|\gamma(\tau)|$ is a periodic function (see Eq. (3)) displaying peaks spatially separated by Y = 50 mm, between the peaks $|\gamma(\tau)| = 0$. According to Eq. (2) this $|\gamma(\tau)|$ allows to obtain interference between object and reference beam only when the path difference $(d_{SRQ} - d_{SPQ})$ is equal to nY, by processing the hologram we are able to reconstruct sections of the object axially separated by $Y/2$. In Fig. 2(b), the intersection lines of the cone with PL-2 and PL-3 are blurred since the reduced depth of focus does not allow to reconstruct sharp profiles located at different planes. Figures 2(c) and 2(d) show that digital focusing of the hologram allows to obtain sharp profile lines at PL-3 and PL-2, respectively. Notice that along with the three rings some unwanted reconstructions are also visible in the figures (in particular in Fig. 2(b) we have an unwanted ring as well, displaced with respect to the center). The artifacts are due to the reflections inside the beamsplitter plate or the camera protection glass, and could be removed by using components with antireflection coatings. The multiple section reconstructions at well-defined axially spaced planes can be obtained only by the fc-laser, and Fig. 2 clearly shows the advantage of using such a light source. A conventional short coherence or a femtosecond laser provides single sectioning only. Only the planes where the reconstructions are focused provide sharp profile lines, and thus the axial location of the intersection between the object and a given plane can be identified by digital focusing.

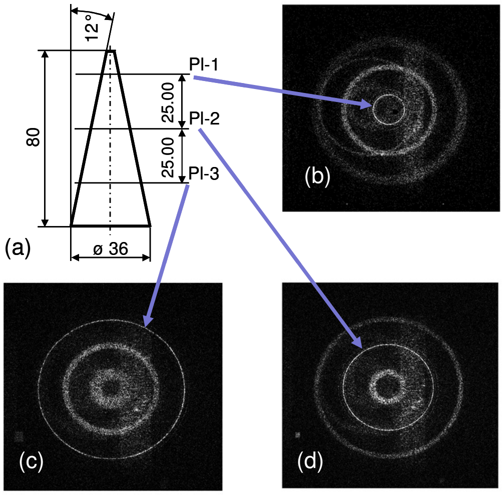

Fig. 2. a) Schematic of the rough metallic cone used for the investigations. b), c), d) Reconstruction of holograms at three different planes separated by 25.00 mm.

The three reconstructed profiles obtained from a single hologram (see Fig. 2) do not allow to get the complete 3-d shape of the object. More sections would be necessary for this purpose which could be obtained by using a fc-laser having larger frequency comb spacing and thus a reduced axial plane separation $Y/2$.

The scanning method was used to obtain more section profiles. The path length of the reference beam was changed by shifting the reference mirror, and a sequence of holograms was recorded. Such holograms allow the reconstruction of different sections of the object. Figure 3 shows the 3-d shape reconstructed from 17 holograms recorded by displacing the reference mirror by 1 mm between each hologram. Each of the 17 holograms contains at least two profile rings (some of them three), for the evaluation only two rings have been used. Due to the limited range of the moving stage (17 mm was the maximum displacement), the data in the reconstructed cone volume between 17 mm and 25 mm are missing. The automatic identification of the profile lines in the reconstructed holograms was done by using threshold filters. We already pointed out that the reconstructed wavefronts contain noise (see e.g. Fig. 2), in some cases this can create difficulties in the identification process of the contour lines. The axial resolution is given by the step of the scanning and thus more holograms are needed for improving the accuracy which is limited by the temporal coherence length of one laser pulse i.e. $c/\Delta\nu \approx 30$ µm. The measurement uncertainty is given by different contributions (set-up geometry, detector noise, unwanted interferences) and was approximately ± 100 µm in our experiment.

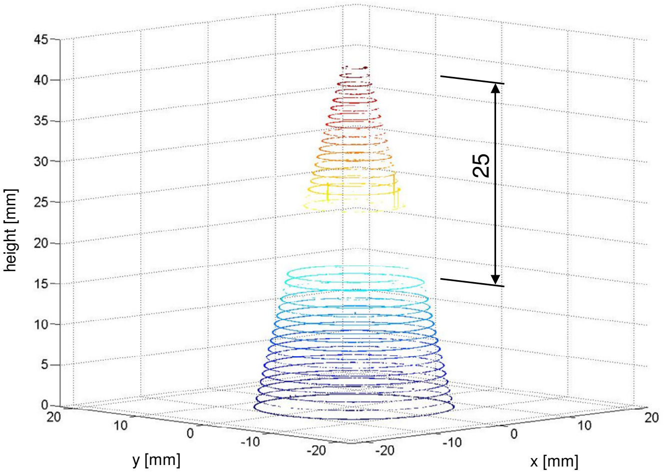

Fig. 3. Numerical reconstruction of a part of the rough metallic continuous cone with a half angle of 12°.

4. Conclusion

The results show that a set-up based on digital holography using a fc-laser can be used for simultaneous multiple optical sectioning, such sectioning cannot be obtained by any other holographic method. Here the measurement time can be reduced by a factor k, where k is the number of the reconstructed sections in one hologram. In the next few years, we expect the availability of fc-lasers based on microresonators [11,12] with larger frequency spacing $\Delta\nu_{fc}$ in the range of 1 THz. In this case the distance $(Y/2)$ of the sectioning can be reduced to the 100 µm range. This will allow us to use the optical sectioning method for technical and biological applications in microscopy. New developments of fc lasers will allow us to change the frequency spacing by tuning the Fabry Perot cavity in the laser system; this will help us to avoid the scan in the reference arm. Furthermore, by using powerful frequency comb lasers [22], the multilevel optical sectioning method can also be extended to larger objects which may be located far away from the detecting system (airplanes, buildings or power plant components). The principle of dual frequency comb holography [19] can make a contribution to absolute 3-d measurements. By using micro-optical elements or optical fibers, a rather compact setup can be built.

Acknowledgment

The authors would like to thank Mr. Andreas Lorenz for skilled manufacturing of the test object.

#161359 - $15.00 USD Received 11 Jan 2012; revised 23 Feb 2012; accepted 12 Mar 2012; published 14 Mar 2012